Ph.D. Thesis

Structural and photocatalytic investigations of TiO_2-MoO_3 composites

Kedves Endre-Zsolt

Supervisor:

Prof. Univ. Dr. habil. Lucian Baia

Babeș-Bolyai University

Cluj-Napoca, Romania

Babeș-Bolyai University

2022

Contents

Introduction

Advanced oxidation processes (AOPs) are fast developing technologies in waste water treatment, these processes include Fenton reactions [1], ozonation [2], based on γ-radiolysis or UV_{254nm} or VUV_{185nm} photolysis [3], and heterogeneous photocatalysis [4]. Photocatalysis is a prominent process which is widely studied since there are basically infinite numbers of catalysts that can be investigated in this process. However, the goal is to achieve catalysts with high performance under sunlight irradiation, which means mostly visible-light-induced catalysts. Latest studies show that TiO_2 is still one of the most performant catalyst in UV light [5], while MoO_3 is presented as a promising visible light induced photocatalyst [6]. Combining catalysts can lead to increase the photocatalytic efficiency and shifting the activation energy towards lower energy requirements [7].

Hydrothermal crystallization is a very popular process that can be used to precipitate shape tailored nanocrystals [8-10]. The parameters are easily adjustable and also the concentration of the precursor, the capping agent or of any other additive can be easily regulated. By this the crystallization process can be influenced and different structural properties can be achieved, like the morphology, the crystal phase, specific surface area, doping the crystal. All these parameters can have affected by the synthesis parameters and consequently also affect the photocatalytic activity of the semiconductor.

TiO_2 was the semiconductor I started my research with, respect to this I wanted to expand my knowledge and immerse myself in the characterization of semiconductors. In 2017, Fujishima himself addressed the young researchers that fundamental research is still needed to make this process effective [11]. TiO_2 is widely studied and a lot of data is available for researchers since 1983 in the topic of heterogeneous photocatalysis [12-14], but there are still questions and fields that are scarcely studied like: whether is there any connection between the morphology and the TiO_2 photocatalytic activity; why there are semiconductors with the same structural and optical properties but different photocatalytic efficiency. The second question was also raised by Bunsho Ohtani who concluded that inactivity could be caused by many reasons while active catalysts are all the same. "*happy (active) photocatalysts are all alike; every unhappy (inactive) photocatalyst is unhappy in its own way*"[15].

MoO_3 exists in a variety of crystal phases but the following three are mostly used: orthorhombic (α-MoO_3), hexagonal (h-MoO_3), monoclinic (β-MoO_3) [16]. Out of three, orthorhombic phase is the most stable thermodynamically and popular as a visible light induced photocatalyst. However, the literature presented many times that α-MoO_3 is an efficient adsorbent for RhB and MB [17]. Therefore, ambiguity is present in

the literature, because most articles assess α-MoO_3 photocatalytic activity with the degradation of RhB or MB [18, 19]. Besides its promising photocatalytic and adsorptive properties, it is also known as a promising sensor for different organic molecules[20]. These features drawn my attention to make photocatalysts that can work under visible light irradiation and simultaneously can be used as a sensor, to monitor the presence of a pollutant in aqueous medium.

The main objectives of the present PhD thesis

My main goal was to obtain photocatalytically active TiO_2 and MoO_3 that I can mix and form binary composites. TiO_2 is far known as the pioneer of photocatalysis with the highest catalytic efficiency, MoO_3 is a very promising semiconductor due to its optical properties that makes it possible to utilize the visible light in photocatalysis. Moreover, structural changes can occur in MoO_3 ensuring that it can be also used as a sensor during these processes. Combining the widely known TiO_2 and the promising MoO_3 could store potentials to increase the overall efficiency, to decrease the activation energy, and to be as an organic compound sensor. Therefore, I studied both of these oxides' crystallization procedure and their application in advanced oxidation processes.

The theses structure

1. Synthesis of shape tailored TiO_2 nanostructures

Solvothermal synthesis of TiO_2 from TTIP, TBU, and $TiCl_4$

Structural and Optical characterization of TiO_2 crystals

Photocatalytic efficiency assessments of TiO_2 nanostructures in UV light (MO, SA)

Investigation of SA and its intermediates photocatalytic degradation kinetics concerning the pollutant concentration, catalyst load, and light intensity.

2. Synthesis of shape tailored MoO_3 nanostructures

Hydrothermal synthesis of α-MoO_3 and h-MoO_3

Calcination of commercial α-MoO_3

Structural and optical characterization of MoO_3 crystals

Photocatalytic assessment of α-MoO_3 and h-MoO_3 crystals (anionic and cationic dyes)

- Adsorption assessment of anionic and cationic dyes on α-MoO_3 as a function of structural properties
- Relation of the cationic dyes structure and α-MoO_3 structure.

3. Investigation of α-MoO_3 as a co-catalyst in photocatalytic experiments next to various photocatalysts

- Preparation of composites with active photocatalysts (TiO_2, AgBr, ZnO, BiOI, Cu_2O)
- Structural and optical investigation of the composites
- Evaluation of the composites' photocatalytic activity and the inhibitive effect of α-MoO_3 upon them

4. Inhibition effect of α-MoO_3 over Fenton reactions

- Calcination of AMT and recrystallization of the obtained α-MoO_3 via hydrothermal treatment
- Structural characterization of α-MoO_3 crystals
- Demonstration of the inhibitor property of α-MoO_3

Synthesis of shape tailored hierarchical TiO_2

Two TiO_2 samples series were prepared *via* hydrothermal crystallization, one from Tetraisopropyl orthotitanate (TTIP, reagent grade 97%, MERCK) the other one from Tetrabutyl orthotitanate (TBU, reagent grade 97% Aldrich) precursors. First an aqueous precursor solution ($TTIP_{aq}$ or TBU_{aq}) was prepared and that contained the following: chosen precursor (TTIP or TBU), hydrochloric acid, distilled water, and hexadecyltrimethylammonium bromide (CTAB, Aldrich). For further shape tailoring this aqueous solution was mixed with ethylene glycol and in the very last case with urea. The synthesis was made at two different precursor concentrations and hydrothermal crystallization was carried out at two different temperatures. In total 24 samples have been made. The next figure summarizes all the samples that were made and compared during the investigation.

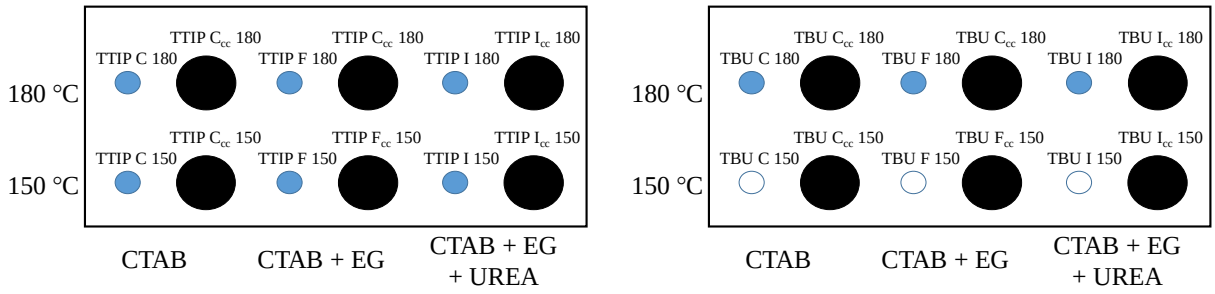

Figure 1. Summarizes the TTIP and TBU samples

TiO_2 with the best photocatalytic activity that I made was synthesized from $TiCl_4$. The synthesis has been carried out in an autoclave in hydrothermal conditions as the above-mentioned TBU and TTIP samples, but different capping agents were used. The molar ratio applied during the synthesis was:

$TiCl_4$:SDS:thiourea:HCl:H_2O = 1:2:10:11:300. A highly viscous solution was made and transferred into a Teflon-coated autoclave which was heated up to 180 °C for 24 h. The washed and dried precipitate was used in photocatalytic experiments of SA degradation, where the kinetics were also discussed.

Preparation of MoO_3 with different structural properties

As TiO_2, several MoO_3 samples were made in different hydrothermal conditions to obtain shape tailored crystallized oxide that can be investigated in photocatalytic experiments. 1 g ammonium molybdate tetrahydrate (AMT) $(NH_4)_6Mo_7O_{24}{\cdot}4H_2O$ was dissolved in 90 mL 1 M acid (HCl, HNO_3, or H_2SO_4) and it was stirred for 60 min at 500 rpm and room temperature. The obtained solution was poured into a stainless-steel autoclave and was placed into an electric furnace where the hydrothermal crystallization occurred. The crystallization was carried out using two different parameter sets. The first sample series, called (*MoO_3 L-"acid"*), was crystallized for 3 h long at 120 °C, while the second sample series, called (*MoO_3 H-"acid")* for 20 hours and at 180 °C. These samples were used in photocatalytic and adsorption experiments.

Commercial α-MoO_3 (99.5%, Alfa Aesar, Molybdenum(VI) oxide) was used as a reference catalyst. Furthermore, 2g of it was treated at different calcination temperatures (250, 300, 400, 500, and 750 °C) which resulted samples with uniform crystal phase but different crystal facet. The samples produced by this method are named as follows: "α-MoO_3 (applied temperature)". Using these samples, the α-MoO_3 prominent adsorption feature was presented, and its inhibition effect upon TiO_2.

In my last study I treated thermally the AMT at different temperatures (250, 300, 400, 500, and 750 °C) to obtain α-MoO_3 with different crystalline facet ratio. The well crystallized samples were further treated in a hydrothermal process where in the presence of H_2O_2 and high temperature peroxo molybdates have been formed. During hydrothermal process recrystallization has taken place and MoO_3 formed again with different crystalline structure. These samples were used to inhibit the Fenton reactions.

$$2MoO_3 + 8H_2O_2 \rightarrow 2MoO_2(OH)(OOH) + 6H_2O + 3O_2 \quad (1)$$

$$2MoO_2(OH)(OOH) \rightarrow 2MoO_3 + 2H_2O + O_2 \quad (2)$$

Methods and Instrumentation

X-ray powder diffraction (XRD)

The as-prepared crystals' diffractograms were registered with a Shimadzu 6000 diffractometer using Cu-K_α radiation (λ = 1.5406 Å) at 40 kV and 30 mA which possessed a graphite monochromator. The crystal phase was determined using POW_COD database in QualX software. The average size of the crystals was estimated using the well-known Scherrer equation [21, 22].

UV-vis spectroscopy

The quantitative analysis of the MO, and SA during photocatalytic investigations, and the adsorption for was carried out using an Analytic Jena Specord 250 plus UV-Vis spectrophotometer. MO and SA spectra were recorded in the range of 250–650 nm for each sample.

The decolorization rate of MO during Fenton reactions was followed with a UV-Vis spectrophotometer (P4, WVR), by measuring the absorption spectra of the samples between the interval of 250-800 nm.

Diffuse reflectance Spectroscopy (DRS)

The diffuse reflectance spectrum (DRS) of the samples was recorded between 250-800 nm with a JASCO-V650 spectrophotometer with an integration sphere (ILV-724), as a reference $BaSO_4$ was used. The indirect band gap values were estimated by applying the Tauc plot [23].

Fourier Transformed IR spectroscopy (FT-IR)

FT-IR spectrum of the samples was recorded in the range of 400 – 4000 cm^{-1}, with 4 cm^{-1} spectral resolution with a JASCO 4100 spectrometer. The samples (~1.5 mg of TiO_2, ~1.2 mg of MoO_3) were mixed with 200 mg of KBr and pellets were made under 5 bars. For reference measurement, I made pure KBr pellets from 200 mg.

Scanning and Transmission Electron Microscopy (SEM and TEM)

The morphology of the microstructured samples was captured by field emission scanning electron microscope (SEM), Hitachi S-4700 Type II FE-SEM operated at 10 kV. The samples were attached to a carbon adhesive tape which was fixed on an aluminum sample holder.

A FEI Tecnai G2 X-TWIN TEM (200 kV) transmission electron microscope was used to take electron diffraction (ED) patterns and micrographs about the morphology of the MoO_3 particles. A small amount of the examined material was suspended in 1.25 cm^3 of ethanol then a few drops of this suspension were placed and dried onto the surface of a CF 200 Cu TEM grid.

X-ray photoelectron spectroscopy (XPS)

The photoelectron spectroscopy XPS spectra were recorded by using a Specs Phoibos 150 MCD system employed with a monochromatic Al-Kα source (1486.6 eV) at 14 kV and 20 mA, a hemispherical analyzer and, a charge neutralization device. The oxide samples were fixed on a double-sided carbon tape where the powder completely covered the tape. The binding energy scale was charge referenced to the C 1s at 284.8 eV. High-resolution Ti 2p and O 1s spectra were obtained using analyzer pass energy of 20 eV in steps of 0.05 eV for analyzed samples. In the case of molybdenum samples, the contact time with the X-ray radiation was minimized to avoid sample degradation, namely the reduction of Mo(VI) species. Survey spectra were collected with a pass energy of 80 eV and 1 eV step size, high resolution spectra were collected with a pass energy of 40 eV and 0.1 eV step size. The data analysis was carried out with CasaXPS software.

Raman Spectroscopy

Raman measurements were carried out with a Thermo Scientific DXR Raman microscope, equipped with a diode-pumped frequency-doubled Nd:YAG laser with 100 mW maximum power. The sample was irradiated by a laser with a wavelength of 532.2 nm and the measurements were performed with a spectral resolution of 4 cm^{-1} respectively, the spectra were collected in the 50 – 1050 cm^{-1} domains. An area of 5 × 5 μm was used for data acquisition and the integration time was 10 s, accumulations have been done for two times, and laser intensity was 50% of the maximum 100 mW laser intensity.

High performance liquid chromatography (HPLC)

Phenol and salicylic acid concentration was followed using an Agilent 1100 series HPLC equipment. Phenol was followed at 210 nm while salicylic acid at three wavelengths (210, 250, and 298 nm) and the reaction intermediates were separated with an ODS column (length 25 cm, an ODS column is filled with a packing of octadecylsilyl groups). The eluent consisted of methanol and water mixture for both cases. The methanol was 50% (V/V) for phenol and 10% (V/V) for salicylic acid determination.

Zeta potential

The zeta potential (ζ-potential) of α-MoO_3 samples was measured three times with a dynamic light scattering analyzer (Nano ZS90 Zetasizer, Malvern Instruments equipped with a He–Ne laser (633 nm, 5 mW)) and the mean value with its corresponding standard deviation has been presented.

Other investigation methods used during the experiments

The specific surface area values were measured by N_2 adsorption and the Brunauer-Emmet-Teller (BET) approach, using a Sorptomatic 1990 apparatus.

The pH was monitored with a SenTix@980 pH electrode.

The calcination was carried out in an electrical muffle furnace in an ambient atmosphere.

Results and Discussion

Synthesis of shape tailored TiO_2 nanostructures and their photocatalytic assessment [5, 24]

T1. Sensitivity of TiO_2 structural properties to the hydrothermal crystallization parameters

The initial concentration of the solvothermal crystallization parameters (temperature and the capping agents) on the morphology of TiO_2. Despite having the same crystallization process, TBU and TTIP resulted samples with different crystal structure. Only 1 pair of samples resulted in the same crystal structure with subtle differences in their average particle size. The capping agents affect differently the TiO_2 crystallization growth depending from the precursor.

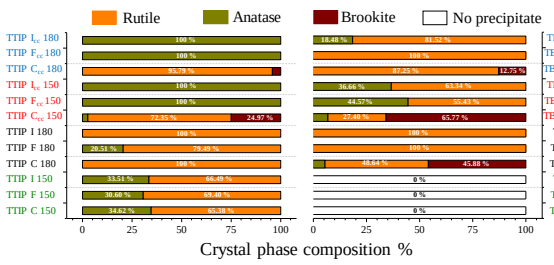

Precursor	C sample crystallite mean size (nm)						F sample crystallite mean size (nm)						I sample crystallite mean size (nm)					
	TTIP			TBU			TTIP			TBU			TTIP			TBU		
Crystal phase	A	R	B	A	R	B	A	R	B	A	R	B	A	R	B	A	R	B
150	47.4	63.4	-	-	-	-	7.0	5.4	-	-	-	-	9.0	6.6	-	-	-	-
180	76.4	-	-	-	80.2	76.1	15.0	9.0	-	-	18.1	-	14.9	-	-	-	20.8	-
150 conc.	37.2	19.4	38.0	-	68.5	26.7	6.1	-	-	6.2	5.7	-	7.1	-	-	5.2	4.7	-
180 conc.	-	29.5	70.8	-	30.1	27.3	11.3	-	-	17.2	-	-	9.1	-	-	7.3	5.9	-

Figure 2. Structural properties of TTIP and TBU samples.

T2. TBU samples possess enhanced photocatalytic activity of compared to TTIP samples with similar structural properties.

TBU and TTIP samples were evaluated photocatalytically with two different pollutants: methyl orange and salicylic acid. Methyl orange decolorization was more efficient with TiO_2 obtained from TBU. However, all the active catalysts decomposed not only MO but the SA with a similar conversion rate. The structural characteristics also proven that TiO_2 formed from TBU more likely formed Ti^{3+} than TTIP, furthermore TTIP samples more readily adsorbed organic matter on their surface thus reducing the ability to be activated.

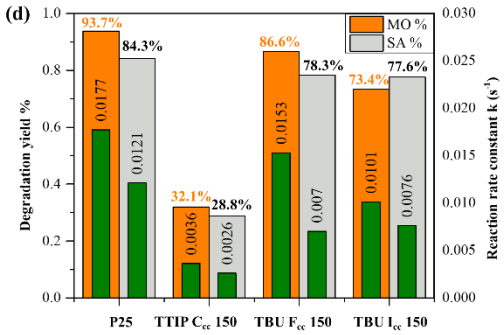

Figure 3. The photocatalytic conversion rate of MO and SA using the most active TiO_2 photocatalysts.

T3. Light intensity influence on SA photocatalytic decomposition, intermediate formation and degradation rate

The decomposition of SA via photocatalytic process was examined in more depth. Varying some of the main parameters, like pollutant initial concentration, catalyst load, and light intensity I investigated the kinetics of the SA decomposition. The catalyst load within the range of 0.5 – 1.25 g $\cdot l^{-1}$ did not affect the rate of the degradation. Different initial pollutant concentration demonstrated that during the photocatalytic decomposition intermediates can accumulate. However, the most fascinating results were measured at different light intensities where the intermediates were followed by spectrophotometer and HPLC as well. The photocatalytic decay curves show that indifferently the light intensity the SA decomposition rate is similar, however the intermediates are produced at different rates and their decomposition is slower than the SA.

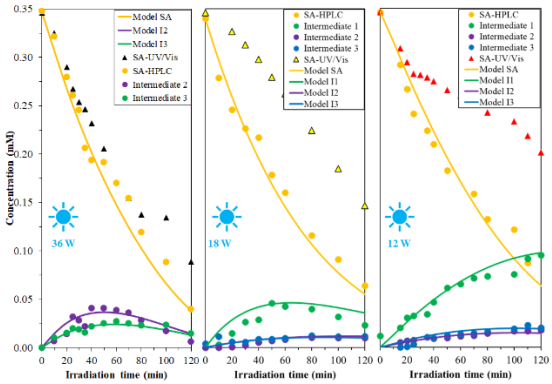

Figure 4. Photocatalytic decomposition of SA and its intermediates at different light intensities in the presence of TiO_2-HT

Synthesis of shape tailored MoO_3 nanostructures and their application as a photocatalyst and adsorbent

T4. Photocatalytic inactivity of h-MoO_3, and α-MoO_3 in the decomposition of organic dyes but prominent adsorption for cationic dyes in the presence of α-MoO_3

Unfortunately, none of the MoO_3 samples shown any sign of photocatalytic efficiency in the decomposition of the next compounds: phenol, oxalic acid, anionic dyes, and cationic dyes. During photocatalytic experiments α-MoO_3 presented prominent adsorption properties towards cationic dyes. Moreover, congo red, which is an anionic dye, had shown adsorption affinity towards **α**-MoO_3 after protonation occurred and disclosed that in the presence of α-MoO_3 acidification occurs.

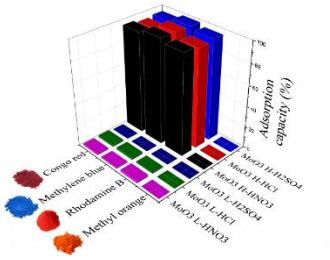

Figure 5. Adsorption capacity of α-MoO_3 samples, assessed with two cationic (RhB and MB) and two anionic (MO and CR) dyes.

T5. Dependence of the adsorption capacity of α-MoO_3 on crystal facet ratio, and variation of its efficiency with contact time.

α-MoO_3 samples with different crystalline facet ratio were made to investigate whether the adsorption is structural dependent. The adsorption capacity was assessed with two cationic dyes, methylene blue and rhodamine B. The setup is presented in Figure 6. This experiment presented that the sample with (040) crystalline facet with the highest specific surface area was the most beneficial in this process. In contrast in a batch adsorption experiment the one with (021) dominant facet presented the highest adsorption capacity.

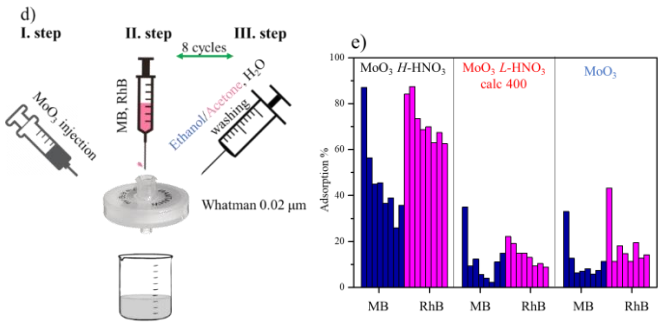

Figure 6. Filtration of cationic dyes (MB and RhB) with α-MoO_3 containing microfilter.

MoO_3 nanostructures inhibits photocatalysts activity

T6. Inhibition of the photocatalytic efficiency of other photocatalysts in the presence of α-MoO_3

α-MoO_3 was mixed mechanically with 5 different active photocatalysts (AgBr, BiOI, ZnO, TiO_2, and Cu_2O). The photocatalytic efficiency was evaluated with the degradation of methyl orange and phenol. The results showed that the most of the photocatalysts were inhibited drastically in the presence of α-MoO_3. This suggested that α-MoO_3 solely will not be an efficient photocatalyst against these pollutants.

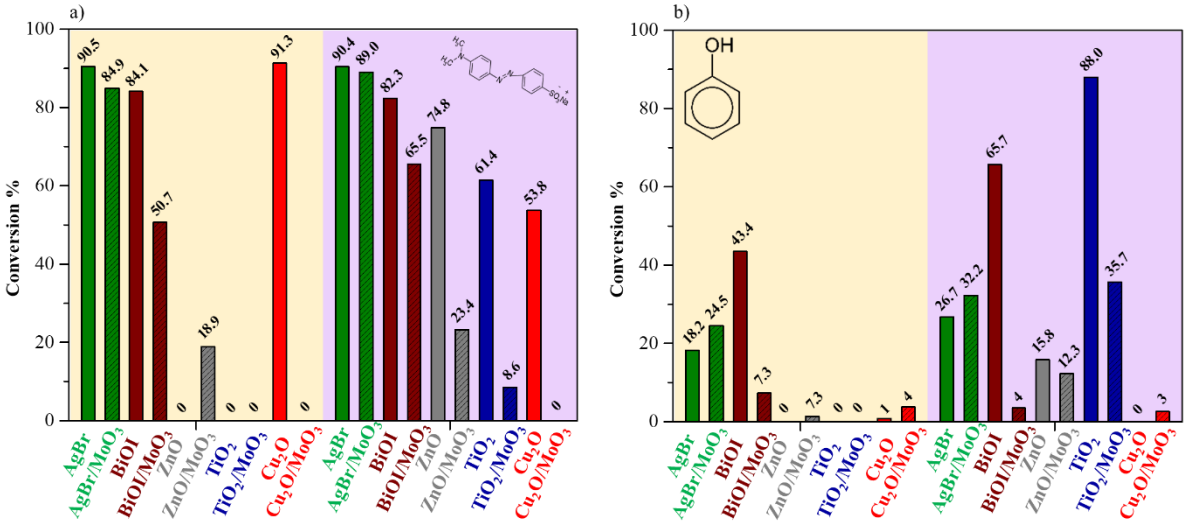

Figure 7. Photocatalytic activity of pristine and their composites with α-MoO_3 was assessed in UV or visible light irradiation by the degradation of methyl orange and phenol.

Adsorption and inhibition of AOPs dependance on α-MoO_3 structural properties[16]

T7. Variation of dye adsorption as a function of pH of aqueous solution and acidification rate as a function of water adsorption on the surface of α-MoO_3.

Commercial α-MoO_3 was heat treated at different temperatures to enhance the (040) crystal facet. The differently structured samples adsorption capacity was assessed using 4 cationic dyes (rhodamine B, methylene blue, crystal violet and malachite green). The presence of α-MoO_3 decreases a solution pH because it is slightly soluble in water, resulting molybdic acid or other types of molybdate anions (such as MoO_4^{2-} or $HMoO_4^-$) causing acidification of the aqueous medium [168]. Following both the pH and the adsorption rate I found that the pH determines the adsorbed amount of dye. The adsorbed amount differs from the structure of the dye but not from the α-MoO_3. The crystal violet had finished at the highest pH, that imply the amine groups clearly increases the adsorption on the surface of α-MoO_3. The α-MoO_3 structure determines the acidification rate, and the pH determines the adsorption so it was proven that the acidification rate determines the adsorption rate. The acidification rate, however, was decreasing as the (040) facet was increasing, where it is known that the water adsorption is not favored. Hence, the samples with (021) showed higher acidification rate than samples with (040) dominant facet.

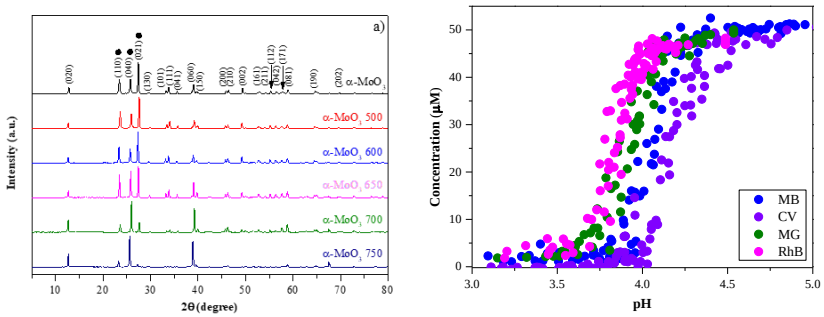

Figure 8. XRD of the differently structured α-MoO_3 obtained via calcination and the adsorption of cationic dyes as a function of pH

T8. Hydrothermal recrystallization of α-MoO_3 in the presence of H_2O_2 as a method to obtain fibrous crystals and facet intensification (040)

Similarly to the previous batch of samples where the commercial α-MoO_3 was heat treated, *via* calcination of AMT (above 400 °C) α-MoO_3 crystals with different structures were obtained. These samples were recrystallized hydrothermally in the presence of H_2O_2 and CTAB to achieve shape tailored crystals. Interestingly, only the morphology and the intensity of the (040) facet have been changed after the recrystallization.

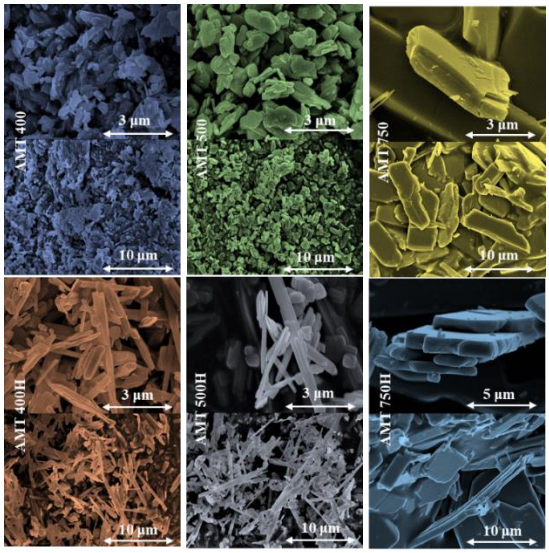

Figure 9. α-MoO_3 samples without well-defined morphology obtained from AMT via calcination and their recrystallized fibrous shape tailored pairs.

T9. Inhibition of photocatalytic and Fenton reactions by the presence of α-MoO_3.

It was presented that α-MoO_3 clearly inhibits photocatalytic degradation independently from the type of the photocatalyst. However, the reason is still not known. Therefore, another process from AOPs was assessed with the degradation of methyl orange in the presence of α-MoO_3 crystals. The Fenton reaction was very effective almost 100% decolorization was achieved, on the other hand α-MoO_3 clearly inhibited this process as the photocatalytic one. During photocatalysis both holes and hydroxyl radicals are formed, Fenton reactions consuming H_2O_2 generate only hydroxyl radicals. Hence, α-MoO_3 is very likely a hydroxyl radical scavenger thereby AOPs can be inhibited in the presence of this oxide. The differently structured α-MoO_3 behaved consistently since the Fenton reactions were similarly inhibited as the photocatalysts as a function of the oxide structure.

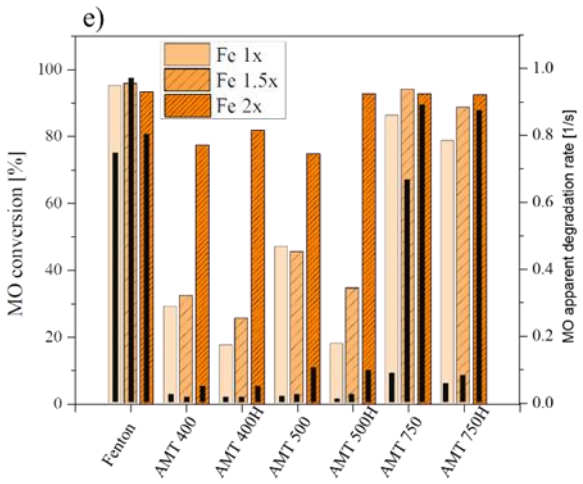

Figure 10. MO conversion and degradation rate *via* Fenton reactions and in the presence of differently structured α-MoO_3.

Conclusion

According to my goals, I have prepared well crystallized TiO_2 and MoO_3 and I have investigated their structural, morphological, and optical properties. The photocatalytic activity was assessed for both semiconductors with the degradation of methyl orange, salicylic acid, and phenol. The adsorption was evaluated only for α-MoO_3 with cationic dyes.

TiO_2 nanostructures disclosed that the formation of TiO_2 is extremely sensitive on the synthesis parameters, resulting distinctive photocatalytic efficiency even for similarly structured crystals. TiO_2 with prominent photocatalytic activity was further examined in the photocatalytic degradation of salicylic acid. Hereby, the external parameters were studied like light intensity, catalyst load, and pollutant concentration. The light intensity changes disclosed that the SA degradation rate subtly affected by this parameter, however formation and degradation rates of the intermediates are determined and change with this parameter.

Regarding MoO_3, the morpho-structural and optical characterizations have been carried out similarly as it was done for TiO_2. Unfortunately, the MoO_3 did not show photocatalytic activity in the degradation of several organic compounds. However, orthorhombic MoO_3 phase presented prominent adsorption properties towards cationic dyes, which is deceptive since these dyes were used frequently in the Literature to assess the photocatalytic activity of MoO_3 in visible light irradiation. This adsorption was studied meticulously with differently structured α-MoO_3. It was found that the crystalline facets of α-MoO_3 determines the adsorption rate while the structure of the dye defines at what pH the adsorption starts.

The photocatalytic activity of α-MoO_3 has been examined in composites with different photocatalysts. The activity of the pristine photocatalysts were established by the degradation of MO and phenol. In all cases, the α-MoO_3 inhibited the photocatalysts activity leading to conclude that MoO_3 can inhibit the AOPs. Therefore, another set of α-MoO_3 samples has been made with different crystalline facet ratio *via* calcination and recrystallization with hydrothermal process. The recrystallization of α-MoO_3 successfully influenced the morphology and increased the (040) facet. As the photocatalytic treatment, the Fenton process was also inhibited by the α-MoO_3 samples. The inhibitive effect was decreasing as the (040) facet increases, while the adsorptive effect occurs opposite. Since the Fenton reaction degrades organic compounds by the presence of hydroxyl radicals, which is inhibited in the presence of α-MoO_3, I think that α-MoO_3 should be a hydroxyl radical scavenger which is structural dependent.

Scientific Activity

Scientific Papers:

Papers related to the Ph.D. program

1. **E. Z. Kedves**, Z Pap, K Hernadi, L Baia

"*Significance of the surface and bulk features of hierarchical TiO_2 in their photocatalytic properties*"

Ceramics International, 2021

I.F.: 5.16 AIS: 0.552

Cited: 6 (Google Scholar)

2. **E. Z. Kedves**, I. Székely, L. Baia, M. Baia, A. Csavdári, Z. Pap

"*The Comparison of the Photocatalytic Performance Shown by TiO_2 and TiO_2/WO_3 Composites—A Parametric and Kinetic Study*"

Journal of Nanoscience and Nanotechnology, 2019

I.F.: 1.134 AIS: 0.142

Cited: 5 (Google Scholar)

3. **E. Z. Kedves**, E. Bárdos, T. Gyulavári, Z. Pap, K. Hernadi, L. Baia

"*Dependence of cationic dyes' adsorption upon α-MoO_3 structural properties*"

Applied Surface Science, 2022

I.F.: 7.392 AIS: 0.848

Cited: 9 (Google Scholar)

4. **E.-Z. Kedves,** C. Fodor, Á. Fazekas, I. Székely, Á. Szamosvölgyi, A. Sápi, Z. Kónya, L. C. Pop, L. Baia, Zsolt Pap

"*α-MoO_3 with inhibitive properties in Fenton reactions and insights on its general impact on OH radical based advanced oxidation processes*"

Applied Surface Science, 2023

I.F.: 7.392 AIS: 0.848

Submitted Paper

5. **E. Z. Kedves**, E. Bárdos, A. Ravasz, Zs.-R. Tóth, Sz. Mihálydeákpál, Z. Kovács, Z. Pap, L. Baia

"*Photoinhibitive properties of α-MoO_3 on its composites with TiO_2, ZnO, BiOI, AgBr, and Cu_2O*"

Materials, 2023

I.F. 3.748 AIS: 0.541

Cumulative I.F.: 21.078; **Cumulative AIS: 2.39**

Expected: *Cumulative I.F.: 24.826;* *Cumulative AIS: 2.931*

Other Papers:

1. Székely, **E. Z. Kedves**, Z. Pap, M. Baia

"*Synthesis Design of Electronegativity Dependent WO_3 and $WO_3 \cdot 0.33H_2O$ Materials for a Better Understanding of TiO_2/WO_3 Composites' Photocatalytic Activity*"

Catalysts, 2021

I.F.: 4.501

Cited: 5 (Google Scholar)

2. E. Bárdos, V.A. Márta, S. Fodor, **E. Z. Kedves**, K. Hernadi, Z. Pap

"*Hydrothermal Crystallization of Bismuth Oxychlorides (BiOCl) Using Different Shape Control Reagents*" **Materials**, 2021

I.F.: 3.748

Cited: 6 (Google Scholar)

3. C. Cadar, C.I. Fort, A. Mihis, **Zs. Kedves**, K. Magyari, L. Baia, M. Baia, M.C. Dudescu, I. Olteanu, L.C. Cotet, V. Danciu

"*3-Aminopropyl-Triethoxysilane Functionalized Graphene Oxide for Silane-Based Consolidation Treatments to Increase Mortar Performances*"

Journal of Nanoscience and Nanotechnology, 2021

I.F.: 1.134

Cited: 0 (Google Scholar)

4. E. J. Sisay, Sz. Kertész, Á. Fazekas, Z. Jákói, **E. Zs. Kedves**, T. Gyulavári, Á. Ágoston, G. Veréb, Zs. László

"Application of $BiVO_4/TiO_2$/CNT Composite Photocatalysts for Membrane Fouling Control and Photocatalytic Membrane Regeneration during Dairy Wastewater Treatment"

Catalysts, 2023

I.F.: 4.501

Cited: 0 (Google Scholar)

Publications before Ph.D. studies

L. Baia, E. Orbán, S. Fodor, B. Hampel, **E. Z. Kedves**, I. Székely, É. Karácsonyi, B. Réti, P. Berki, A. Vulpoi, K. Magyari, A. Csavdári, C. Bolla, V. Coșoveanu, K. Hernádi, M. Baia, A. Dombi, V. Danciu, G. Kovács, Z. Pap

"Preparation of TiO_2/WO_3 composite photocatalysts by the adjustment of the semiconductors' surface charge"

Materials Science in Semiconductor Processing, 2016

I.F.: 2.593

Cited: 40 (Google Scholar)

Krisztina Vajda, K Saszet, **E. Zs. Kedves**, Zs Kása, V Danciu, L Baia, K Magyari, K Hernádi, G Kovács, Zs Pap

"*Shape-controlled agglomeration of TiO_2 nanoparticles. New insights on polycrystallinity vs. single crystals in photocatalysis*"

Ceramics International, 2016

I.F.: 3.27

Cited: 34 (Google Scholar)

Total Cumulative I.F.: 33.433

Conference Participations

Ph.D. related conferences

1. **Kedves Endre-Zsolt**, Ravasz Alpár, Dr. Kovács Gábor, Dr. PAP Zsolt, Dr. Alexandra Csavdari, Dr. Hernádi Klára, Dr. Lucian Baia "*Kinetic study of the photocatalytic degradation of salicylic acid by different TiO_2 photocatalysts*" XXII. International Conference on Chemistry, November 3-6, 2016, Timișoara, Romania – *Oral presentation*

3. **Endre-Zsolt Kedves**, Lucian Baia, Klára Hernádi, Zsolt Pap "*Hydrothermal synthesis of hierarchical TiO_2 nanostructures and their photocatalytic performance*" Environmental Applications of Advanced Oxidation Processes, June 25-29, 2017, Prague, Czech – *Poster*

5. **Kedves Endre-Zsolt**, Ravasz Alpár, Kovács Gábor, Lucian Baia, Pap Zsolt „*Hierarchical TiO_2 photocatalysts performance investigation based on structural and optical properties*" XXIII. International Conference on Chemistry, October 25-28, 2017, Deva, Romania – *Oral presentation*

6. Ravasz Alpár, **Kedves Zsolt**, Kovács Gábor, Pap Zsolt, Hernádi Klára, Lucian Baia „*Synthesis and photocatalytic activity of binary MoO_3 and TiO_2 composite systems*" XXIII. International Conference on Chemistry, October 25-28, 2017, Deva, Romania – *Poster*

7. **Kedves Endre-Zsolt**, Ravasz Alpár, Pap Zsolt, Lucian Baia, „*Photocatalytic degradation of anionic and cationic dyes with MoO_3 nanocrystals*" Societatea Muzeului Ardelean, ETK-17, November 24-25, 2017, Cluj-Napoca, Romania – *Oral presentation*

8. **Endre-Zsolt Kedves**, Lucian Baia "*Investigation the adsorption and photocatalitycactivity of MoO_3 with cationic and anionic dyes*"-Márton Áron Special College PhD Conference, April 6, 2018, Debrecen, Hungary – *Oral presentation*

9. Alpár Ravasz, **Endre-Zsolt Kedves**, Gábor Kovács Zsolt Pap, Csaba Pajzs, Lucian Baia "*Adsorption of anionicand cationic dyes based on the structural properties of MoO_3*", 15th International Conference "Students for Students", April 21,2018, Cluj-Napoca, Romania – *Oral presentation*

10. **Endre-Zsolt Kedves**, Pap Zsolt, Hernádi Klára, Lucian Baia "*Uncovering the adsorption of organic pollutants on α-MoO_3 with different crystallographic plane ratios*" 12th International Conference on Physics of Advanced Materials, September 27, 2018, Heraklion, Greece – *Oral presentation*

11. Ravasz Alpár, **Kedves Endre-Zsolt**, Tóth Zsejke-Réka, Bárdos Enikő, Fodor Szilvia, Kovács Zoltán, Pap Zsolt, Hernádi Klára, Lucian Baia „*Effect of MoO_3 on the activity of AgBr, BiOI, Cu_2O, and ZnO*" XXIV. International Conference on Chemistry, October 24-27, 2018, Sovata, Romania – *Poster*

12. **Kedves Endre-Zsolt**, Ravasz Alpár, Pap Zsolt, Hernádi Klára, Lucian Baia "*Adsorption of cationic dyes on orthorhombic α-MoO_3*" XXIV. International Conference on Chemistry, October 24-27, 2018, Sovata, Romania – *Oral presentation*

13. **Kedves Endre-Zsolt**, Lucian Baia, "*Kationos színezékek adszorpciója különböző kristályoldalú ortorombos α-MoO_3-al*" Márton Áron Special College PhD Conference, 2019, May 4, 2019, Pécs, Hungary – *Oral presentation*

14. Alpár Ravasz, **Endre-Zsolt Kedves**, Zsejke-Réka Tóth, Enikő Bárdos, Szilvia Fodor, Zoltán Kovács, Zsolt Pap, Klára Hernádi, Lucian Baia "*Photocatalytic investigation of AgBr, BiOI, Cu_2O and ZnO*

semiconductors' binary composites with orthorhombic MoO_3" Environmental Applications of Advanced Oxidation Processes – 6, June 26-30, 2019, Portorose, Slovenia – *Poster*

15. **Kedves Endre-Zsolt**, Ravasz Alpár, Pap Zsolt, Kovács Gábor, Hernádi Klára, Lucian Baia "*Investigation of cationic dyes adsorption on orthorhombic MoO_3 nanocrystalline systems*" Environmental Applications of Advanced Oxidation Processes – 6, June 26-30, 2019, Portorose, Slovenia – *Poster*

16. Ravasz Alpár, **Kedves Endre-Zsolt**, Tóth Zsejke-Réka, Bárdos Enikő, Fodor Szilvia, Kovács Zoltán, Pap Zsolt, Hernádi Klára, Lucian Baia "*Investigation of α-MoO_3 Containing in Binary Composite Systems Photocatalytic Performance*" XXV. International Conference on Chemistry, October 24-26, 2019, Cluj-Napoca, Romania – *Poster*

17. **Kedves Endre-Zsolt**, Fodor Claudiu, Pap Zsolt, Hernádi Klára, Lucian Baia "*Adsorption of Organic Dyes by α-MoO_3: Effect of the Crystal Structure in the Adsorption Process*" XXV. International Conference on Chemistry, October 24-26, 2019, Cluj-Napoca, Romania – *Oral presentation*

18. Fodor C., **Kedves E.-Z.**, Székely I., Pop L.-C., Baia L. "*Preparation of α-MoO_3 with different crystallographic plane ratios: study of the adsorption process using organic dyes*" 9th European Young Engineers Conference, April 24, 2021, Warsaw, Poland – *Online presentation*

Other conferences

1. Ravasz Alpár, **Kedves Zsolt**, Kása Zsolt, Kovács Gábor, Pap Zsolt, Magyari Klára, Hernádi Klára, Lucian Baia "Synthesis and Photocatalytic Activity of Ternary $BiVO_4$, TiO_2, and WO_3 Composite Systems", XXII. International Conference on Chemistry, November, 3-6, 2016, Timișoara, Romania – *Poster*

2. Saszet Kata, **Kedves Zsolt**, PAP Zsolt, Kovács Gábor, Virginia Danciu, Magyari Klára, DombiAndrás, Hernádi Klára, Lucian BAIA „*Investigation of photodegratadion intermediates using TiO_2-based nanostructures*" XXII. International Conference on Chemistry, November 3-6, 2016, Timișoara, Romania – *Poster*

3. Ravasz Alpar, **Kedves Endre-Zsolt**, Pap Zsolt „*The photocatalytic activity of ternary TiO_2-WO_3-$BiVO_4$ composite systems and the optimization of the composite component ratios*" XVIII.

Scientific Student Conference on Technical Sciences (MTDK), April 27-29, 2017, Timișoara, Romania (*Premiul lII.*) – *Oral presentation –Supervisor*

4. Alpár Ravasz, **Endre-Zsolt Kedves**, Zsolt Kása, Lucian Baia, Zsolt Pap "*Hydrothermal synthesis and photocatalytic activity of ternary $BiVO_4$, TiO_2, and WO_3 composite systems*" Environmental Applications of Advanced Oxidation Processes, June 25-29, 2017, Prague, Czech – *Poster*

5. K. Saszet, **Zs. Kedves**, Zs. Pap, Zs. Kása, G. Kovács, V. Danciu, K. Magyari, A. Dombi, K. Hernádi, L. Baia "*Study of photodegratadion intermediates using specific TiO_2-based nanostructures*" Environmental Applications of Advanced Oxidation Processes, June 25-29,2017, Prague, Czech – *Poster*

6. Gábor Veréb, Krisztina Vajda, Zsolt Kása, **Zsolt Kedves**, Kata Saszet, Klára Hernádi, Zsolt Pap "*Preparation and characterization of „TiO_2-C" hybride materials*" Environmental Applications of Advanced Oxidation Processes, June 25-29,2017, Prague, Czech – *Poster*

7. Ravasz Alpar, **Kedves Endre-Zsolt**, Pap Zsolt „*The photocatalytic activity of ternary TiO_2-WO_3-$BiVO_4$ composite systems and the optimization of the composite component ratios*" 34nd National Scientific Students' Associations Conference, March 23, 2019, Budapest, Hungary – *Oral presentation, Supervisor*

References

[1] S.A. Walling, W. Um, C.L. Corkhill, N.C. Hyatt, npj Materials Degradation, 5 (2021) https://doi.org/10.1038/s41529-021-00192-3
[2] L. Prieto-Rodriguez, I. Oller, N. Klamerth, A. Aguera, E.M. Rodriguez, S. Malato, Water Res, 47 (2013) 1521-1528 https://doi.org/10.1016/j.watres.2012.11.002
[3] G. Rózsa, M. Náfrádi, T. Alapi, K. Schrantz, L. Szabó, L. Wojnárovits, E. Takács, A. Tungler, Appl Catal B-Envirom, 250 (2019) 429-439 https://doi.org/10.1016/j.apcatb.2019.01.065
[4] K. Vajda, K. Saszet, E.Z. Kedves, Z. Kása, V. Danciu, L. Baia, K. Magyari, K. Hernádi, G. Kovács, Z. Pap, Ceram Int, 42 (2016) 3077-3087 https://doi.org/10.1016/j.ceramint.2015.10.095
[5] E.-Z. Kedves, Z. Pap, K. Hernadi, L. Baia, Ceram Int, 47 (2021) 7088-7100 https://doi.org/10.1016/j.ceramint.2020.11.061
[6] M. Pérez-González, M. Morales-Luna, J. Santoyo-Salazar, H. Crotte-Ledesma, P.E. García-Tinoco, S.A. Tomás, Catal Today, 360 (2021) 138-146 https://doi.org/10.1016/j.cattod.2019.06.003
[7] L. Baia, E. Orbán, S. Fodor, B. Hampel, E.Z. Kedves, K. Saszet, I. Székely, É. Karácsonyi, B. Réti, P. Berki, A. Vulpoi, K. Magyari, A. Csavdári, C. Bolla, V. Coșoveanu, K. Hernádi, M. Baia, A. Dombi, V.

Danciu, G. Kovács, Z. Pap, Mat Sci Semicon Proc, 42 (2016) 66-71 https://doi.org/10.1016/j.mssp.2015.08.042
[8] I. Székely, G. Kovács, L. Baia, V. Danciu, Z. Pap, Materials, 9 (2016) 258 https://doi.org/10.3390/ma9040258
[9] E. Bardos, V.A. Marta, S. Fodor, E.Z. Kedves, K. Hernadi, Z. Pap, Materials (Basel), 14 (2021) https://doi.org/10.3390/ma14092261
[10] C.M. Zoltán Kovács, Urška Lavrencic Štangar, Vasile-Mircea Cristea, Zsolt Pap, Klara Hernadi and Lucian Baia, Nanomaterials, 11 (2021) https://doi.org/10.3390/nano11051334
[11] P.V. Kamat, ACS Energy Letters, 2 (2017) 1586-1587 https://doi.org/10.1021/acsenergylett.7b00483
[12] T. Gyulavári, Z. Pap, G. Kovács, L. Baia, M. Todea, K. Hernádi, G. Veréb, Catal Today, 284 (2017) 129-136 https://doi.org/10.1016/j.cattod.2016.11.012
[13] P. Wang, C. Jia, J. Li, P. Yang, J Aalloy Compd, 780 (2019) 660-670 https://doi.org/10.1016/j.jallcom.2018.11.398
[14] C.-L.L. Chen-Yung Hsiao, David F.Ollis, Journal of Catalysis, 82 (1983) 418-423 https://doi.org/https://doi.org/10.1016/0021-9517(83)90208-7
[15] B. Ohtani, M. Takashima, Catal Sci Techno, 12 (2022) 354-359 https://doi.org/10.1039/d1cy01955d
[16] E.-Z. Kedves, E. Bárdos, T. Gyulavári, Z. Pap, K. Hernadi, L. Baia, Appl Surf Sci, 573 (2022) 151584 https://doi.org/10.1016/j.apsusc.2021.151584
[17] N. Kumar, R. Kumar, Mater Chem Phys, 275 (2022) 125211 https://doi.org/10.1016/j.matchemphys.2021.125211
[18] Y. Liu, P. Feng, Z. Wang, X. Jiao, F. Akhtar, Sci Rep, 7 (2017) 1845 https://doi.org/10.1038/s41598-017-02025-3
[19] B. Zheng, Z. Wang, X. Wang, Y. Chen, J Hazard Mater, 378 (2019) 120753 https://doi.org/10.1016/j.jhazmat.2019.120753
[20] R. Malik, N. Joshi, V.K. Tomer, Materials Advances, 2 (2021) 4190-4227 https://doi.org/10.1039/d1ma00374g
[21] P. Scherrer, Göttinger Nachr. Gesell, 2 (1918) 98-100
[22] A. Patterson, Physical review, 56 (1939) https://doi.org/https://doi.org/10.1103/PhysRev.56.978
[23] P. Makula, M. Pacia, W. Macyk, J Phys Chem Lett, 9 (2018) 6814-6817 https://doi.org/10.1021/acs.jpclett.8b02892
[24] E.Z. Kedves, I. Szekely, L. Baia, M. Baia, A. Csavdari, Z. Pap, J Nanosci Nanotechno, 19 (2019) 356-365 https://doi.org/10.1166/jnn.2019.15792